**NASA TECHNICAL MEMORANDUM**

NASA TM X-71558

NASA TM X-71558



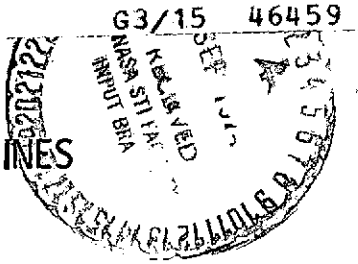

# MAINSHAFT SEALS FOR SMALL GAS TURBINE ENGINES

by Lawrence P. Ludwig
Lewis Research Center
Cleveland, Ohio 44135

and

Peter Lynwander
AVCO-Lycoming Division
Stratford, Connecticut 06497

TECHNICAL PAPER proposed for presentation at
Lubrication Conference cosponsored by the
American Society of Lubrication Engineers and
The American Society of Mechanical Engineers
Montreal, Canada, October 8-10, 1974

# MAINSHAFT SEALS FOR SMALL GAS TURBINE ENGINES

by Lawrence P. Ludwig
National Aeronautics and Space Administration
Lewis Research Center
Cleveland, Ohio 44135

and

Peter Lynwander
AVCO-Lycoming Division
Stratford, Connecticut 06497

E-7983

## ABSTRACT

An experimental evaluation of mainshaft seals for small gas turbine engines was conducted with shaft speeds to 213 m/s (700 ft/sec), air pressures to 148 N/cm$^2$ abs. (215 psia), and air temperatures to 478 K (262° F). A radial face seal incorporating self-acting geometry for lift augmentation was evaluated. In addition, three conventional carbon seal types (face, circumferential segmented, and rotating ring) were run for comparison.

Test results indicated that the conventional seals used in this evaluation may not be satisfactory in future advanced engines because of excessive air leakage. On the other hand, the self-acting face seal was shown to have the potential capability of limiting leakages to one-half that of the conventional face seals and one-fifth that of conventional ring seals. A 150-hour endurance test of the self-acting face seal was conducted at speeds to 145 m/s (475 ft/sec), air pressures to 124 N/cm$^2$ abs. (180 psia), and air temperatures to 408° K (275° F). The seal wear was not measurable. An additional 100 hour of endurance testing at 145 m/s (475 ft/sec) and 148 N/cm$^2$ abs. (215 psia) also revealed non-measurable wear, indicating non-contact operation was achieved at these high rotative speeds (43 200 rpm).

Tolerance to face runout was then demonstrated by a 10 hour run at 0.038 mm (0.0015 in.) face runout at 145 m/s (475 ft/sec); again wear was not measurable, thus indicating gas film separation of the sealing surfaces.

## INTRODUCTION

Mainshaft sealing is becoming increasingly critical in advanced gas turbine engines for helicopters. As shaft speeds, air temperatures, and air pressures increase; engine size has decreased, leaving less envelope to accomplish the sealing function. Advanced

engines in the 1.36 to 4.54 kg/s (3 to 10 lb/sec) class incorporate mainshaft seals that will operate at surface speeds to 137 m/s (450 ft/sec), air pressures to 72 N/cm$^2$ abs. (104 psia), and air temperatures to 810° K (1000° F).

Because of their non-contacting feature, labyrinth seals offer infinite life; however, at high air pressures and temperatures, simple labyrinths will not suffice, and complicated multistage labyrinths must be used. These latter seals incorporate venting and pressurization passages that are costly to produce and difficult to accommodate in small, high-performance engines. Compared with positive-contact seals labyrinths also permit higher airflows, which must be absorbed by the lubrication system. These high airflow (losses) lead to significant performance penalties.

Although the conventional rubbing seal can provide lower leakages, its use at these high speeds, temperatures and pressures is prohibited by its susceptibility to wear under these conditions.

The self-acting seal concept, however, offers the high pressure and speed capability of a labyrinth seal as little or no contact occurs and does provide low leakage of the contact seal because the operating clearance is very small. The self-acting face seal is similar to a conventional face seal except for the added feature of a self-acting geometry (gas lubricated thrust bearing). In operation, the sealing faces are separated a slight amount (in the range of 0.00025 to 0.00127 centimeters, (0.0001 to 0.0005 in.)) by action of the self-acting lift geometry. This positive separation results from the balance of seal forces and the gas film stiffness of the self-acting geometry. The self-acting geometry can be any of the various types used in gas thrust bearings.

Analysis of the self-acting seal concept and experimental feasibility studies for large aircraft gas turbine engines have been detailed in several programs (refs. 1 to 10). The subject program was designed to investigate the operating conditions and problems peculiar to small high-performance helicopter gas turbine engines. Of particular interest was the stability or performance of the self-acting seal operating at high rotative speeds (> 40 000 rpm) where high inertia forces are induced by seal seat face runout.

The experimental evaluation was carried out in a test rig that simulates engine conditions in an advanced gas producer turbine bearing location. All seal and bearing package hardware was lightweight, typical helicopter engine design practice.

In addition to evaluating the self-acting face seal concept, three conventional seal configurations were evaluated. These were the

face, shaft riding, and rotating ring. Data pertaining to airflow, cavity pressure and seal temperature for all seals were developed for a range of speeds and pressures at ambient temperatures. These data provided design criteria and a basis for comparison of the seal configurations. Also an endurance run of the self-acting face seal was conducted.

The specific objectives of the program were to: (a) demonstrate feasibility of operating the self-acting seal at rotative speeds to 50 000 rpm and (b) to obtain a performance comparison to conventional seals.

## APPARATUS AND PROCEDURE

### Rig

The rig bearing compartment (fig. 1) is typical of advanced, high-speed gas turbine packages. Sealing positions were located forward and aft of the bearing, which enabled simultaneously testing of two seal samples.

The prime mover is a 100-horsepower, 20 000 rpm steam turbine. Connecting the steam turbine to the rig is a 3:1 ratio speed increaser. The shaft is supported by a 35-mm, split-inner-race ball bearing in the test position, and by a 25-mm, split-inner-race bearing in the support position. Both bearings are hydraulically mounted, and thrust loading is supplied by coil springs acting on the outer race of the support bearing and pressure differentials across the loading wheel.

A single batch of MIL-L-23699 oil at 367 $\pm$5 K (200 $\pm$10° F) was used throughout the test program. Total oil flow to the bearing compartment was varied with speed to simulate engine conditions. Typical schedule for initial seal evaluation was as follows:

| Shaft speed | | Oil flow | |
|---|---|---|---|
| m/sec | ft/sec | kg/hr | lb/hr |
| 61 | 200 | 54 | 120 |
| 91 | 300 | 81 | 180 |
| 122 | 400 | 108 | 240 |
| 152 | 500 | 136 | 300 |
| 183 | 600 | 162 | 360 |
| 213 | 700 | 189 | 420 |

The bearing was fed by eight 0.81 mm (0.032 in.) jets and each seal face seat cooled by one 0.81 mm (0.032 in.) jet. Oil-in temperature was 366° K (200° F).

The bearing compartment drains by gravity into a static air-oil separator. Desired air pressure is introduced into the cavities adjacent to the test seals, and the air that leaks past the two test seals is passed through a flowmeter from the air-oil separator to obtain a measure of seal leakage.

## Self-Acting Face Seal

The self-acting face seal used in the test program is shown in figure 2. It is similar to a conventional face seal with the addition of the self-acting geometry for lift augmentation.

The primary sealing interface consists of the rotating seal seat, which is keyed to the shaft, and the nonrotating carbon sealing nose assembly, which is free to move in an axial direction, thus accommodating axial motions due to thermal expansion. Sixteen axial springs provide the mechanical force that holds the carbon nose piece in contact with the seal seat during nonrotative periods. The secondary seal, a pressure-balanced carbon piston, is subjected only to the axial motion of the carrier assembly.

Great care is taken to insure flatness of the sealing surfaces after assembly. The seal seat is keyed to the shaft spacer, and is axially clamped by a machined bellows that exerts a predetermined clamping force, thus minimizing distortion of the seal seat. The bellows also acts as a static seal between the seat and the shaft spacer. Cooling oil is passed through the seat to reduce thermal gradients, and the oil dam disc also serves as a heat shield. Windbacks are used to prevent oil from approaching the sealing surfaces.

The depth of the lift pads on the carbon sealing face was measured by taking a proficorder trace across the face. Traces of four of twelve pads were taken before and after each test. The original lift-pad depths typically varied from 0.0153 mm (0.00065 in.) to 0.0250 mm (0.0010 in.).

In operation, the sealing faces are separated slightly, in the order of 0.007 mm (0.0003 in.), by action of the self-acting lift geometry. This positive separation results from the balance of seal forces and the gas film stiffness of the self-acting geometry.

To determine film thicknesses and air leakages in a self-acting face seal, the axial forces acting on the sealing nose piece assembly

must be determined for each operating condition. These forces are the self-acting lift force, the spring force, and the pneumatic forces due to the sealed pressure. Essentially, the analysis requires finding the film thickness for which the opening forces balance the closing forces. When this equilibrium film thickness is known, the leakage rate can be calculated. References 3 through 9 detail the design procedure.

## Rotating Ring Seal

The rotating ring seal (fig. 3) is essentially a close-clearance labyrinth that is free to rotate in the seal case. The rotating ring sealing element is composed of a carbon ring shrunk into a steel retaining band. The retaining band is used to control the expansion rate of the composite ring and to reinforce it against compressive and rotational stress.

The composite ring is designed to have a coefficient of thermal expansion similar to that of the seal runner. The purpose of matching thermal expansion characteristics is to hold a constant clearance (independent of temperature) between the runner outside diameter and the carbon inside diameter.

The composite ring is not restrained from rotating and in operation probably rotates at a speed less than shaft speed. The expansion of the composite ring with speed is utilized to provide a minimum air leakage gap at all operating conditions. If the gap tends to increase, the driving torque decreases and the ring speed decreases. The opposite occurs if the gap decreases: the driving torque increases, the ring speed increases. The seal, therefore, is designed to be self-regulating.

For the test program, the forward seal position was built with a static diametral gap of 0.0610 mm (0.0024 in.) and the aft seal with a static diametral gap of 0.1346 mm (0.0053 in.).

## Circumferential Segmented Seal

The circumferential segmented seal (fig. 4) is a carbon ring consisting of three 120° segments held together by a garter spring on the outside diameter. When the ring is installed on the runner, clearance between the adjacent ends of the segments allows a limited airflow into the bearing cavity. Design clearance, at each gap, is 0.229/0.305 mm (0.008/0.012 in.). During operation, if the carbon wears from shaft contact, the garter spring forces the segments radially inward. When

the clearance between the adjacent carbon segment ends is zero, the ends butt up and the carbon inside diameter no longer contacts the runner. Approximately 0.127 mm (0.005 in.) of radial carbon wear will cause this condition. The seal then operates as a close-clearance labyrinth and the minimum gap is formed at the maximum speed, pressure, and temperature conditions, where the runner is at its largest diameter.

### Conventional Face Seal

The conventional face seal design is shown in figure 5. Seal materials and critical dimensions are listed. The carbon sealing nose is pressure balanced with an area ratio of 0.645 (for pressure balance definition see ref. 4). Pressure balancing is also applied to the secondary carbon piston ring seal both axially and radially. A chromium carbide flame spray is applied to the seat face. The seal was assembled with a 3.02 N (6.8 lb) spring force, which resulted in a calculated primary seal interface pressure of 67 $N/cm^2$ (9.7 psi).

## RESULTS AND DISCUSSION

### Self-Acting Face Seal

Table I contains the gas leakage data for two seals operating over a pressure differential range from 23 to 108 $N/cm^2$ (34 to 156 psi) and a sliding speed range from 91 to 183 m/sec (300 to 600 ft/sec). This is a rotative speed range of 27 300 to 54 600 rpm. Neither the forward nor the aft carbon nose or seal seat showed any wear during this operation. Thus the sealing surfaces were separated by a gas film over the entire matrix of operating variables.

Note in table I that the seal leakage increases as the sliding speed increases (for any given pressure differential). This leakage increase is due to a slight increase of the sealing gap because the increased lift force produced by the lift pads (dynamic effect). As would be expected, the leakage increases as the pressure increases.

To further explore the operating limits of the self-acting seals, 150 hours of endurance operation at ambient temperature was conducted as follows:

| Speed | | Air Pressure | | Time, |
|---|---|---|---|---|
| m/sec | ft/sec | $N/cm^2$ abs. | psia | hr |
| 102 | 334 | 103 | 149.7 | 28 |
| 122 | 400 | 103 | 149.7 | 22 |
| 137 | 450 | 103 | 149.7 | 65 |
| 145 | 475 | 103 | 149.7 | 20 |
| 145 | 475 | 124 | 179.7 | 15 |

Air temperature varied throughout the test but was generally from 372 to 408 K (200 to 275° F).

Seal face plate flatness in the assembled state was measured to be $1.8 \times 10^{-3}$ mm ($70 \times 10^{-6}$ in.) (0.00007 in.). Axial runout was approximately 0.03 mm (0.0012 in.). The seal spring force for the 150 hour test was 31 N (7 lb).

Typical leakage flow results during the 150 hour endurance run are shown in table II for sliding speeds of 137 to 145 m/sec (450 to 475 ft/sec) and for pressure differentials of 93 to 113 $N/cm^2$ (135 to 165 psi). As would be expected, the leakage rate changed with pressure, and there was a slight speed (dynamic) effect, in that the leakage increased as the speed increased.

The aft seal carbon nose wore an average of 0.0044 mm (0.000175 in.) after the first 50 hours, no other wear occurred on the two carbons or face plates during the 150 hour endurance run. Again, these data indicate positive separation of the sealing faces.

## Rotating Ring Seal

Figure 6 summarizes the results of the rotating ring seal tests. Airflow versus pressure differential is plotted for various operating gaps. The operating gaps were calculated at various speeds under the following assumptions or conditions:

1. That the static gaps for both seals were 0.132 mm (0.0052 in.) (based on measurements).

2. The runner is an unsupported thin ring.

3. The thermal growth of the runner and the carbon-metal composite ring are equal.

4. The composite ring does not rotate.

During high speed testing (above 122 m/s (400 ft/sec)) substantial carbon wear occurred. (Wear was to be expected at the 213 m/sec

(700 ft/sec) point, since the calculated diametral operating gap closes to 0.005 mm (0.0002 in.).) This wear causes the data points to trail off the straight line relationship one would expect if wear did not occur, for example, see 213 m/sec (700 ft/sec) [redacted], figure 6.

## Conventional Circumferential Segmented Seal Evaluation

Figure 7 summarizes the circumferential segmented seal test data. It was found during the test program that these seals wore excessively at high speeds and pressures and eventually operated as labyrinths; and figure 7 shows the airflow difference between worn out and new circumferential segmented seals.

## Conventional Face Seal Evaluation

Conventional face seal evaluation covered a range of speeds and air pressures at ambient temperatures. Typical test conditions and resulting airflows, bearing cavity pressures, and seal temperatures are listed in table III. Each run was of 15 minutes duration. Seal temperature was measured at the location shown in figure 5. Only the aft seal was temperature instrumented. The seal operated successfully over a wide range of conditions including 213 m/sec (700 ft/sec) with a pressure difference of 117 $N/cm^2$ (170 psi). Leakage rates, however, were much higher than that of the self-acting seal.

Face seal carbon nose wear was minimal through the test program 0.0051 mm (0.0002 in.) on the forward seal and 0.0102 mm (0.0004 in.) on the aft seal. This wear and the fact that the temperature did not exceed 372 K (210° F) indicate the seals were operating on an air film.

## Comparison of Seal Performance

A comparison of the performance of the various seal configurations is shown in figure 8. In general, the plot shows that self-acting face seal has the potential of significantly reducing (leakage) as compared to the conventional seals.

Of the conventional configurations, face seals allowed the least airflow at high pressure differentials. Circumferential segmented seals are as tight as face seals at moderate operating conditions; however, experience and the subject test program results have shown that at pressure differentials above 41.4 $N/cm^2$ (60 psi) and speeds above 107 m/sec (350 ft/sec), circumferential segmented seals wear out and finally operate as labyrinths. In that case there is little to choose between circumferential, rotating ring, and labyrinth seals in terms of airflows.

Several problems can occur as a result of high airflow into the lubrication system:

1. The air-oil separation system may not be able to handle the volume of air, and accessory gearbox pressure will increase and back pressure the bearing cavities which are in low pressure areas of the engine, causing oil leakage.

2. Depending on the scavenge area of the bearing cavity and the pressure downstream, excessive airflow can pressurize the bearing cavity and limit the oil flow into it, thereby precipitating bearing failure.

3. Excessive hot air flowing into the bearing cavity can degrade the lubricant and be detrimental to the bearings.

To gain some perspective of the magnitude of airflow under discussion, engine experience has shown that excessive airflow into a bearing package incorporating seals of the size used in the test program would be in the order of 0.012 kg/sec (0.029 lb/sec). Taking midpoint values of the range of pressure differentials in figure 9 the face seal could not meet this criterion at pressure differentials above approximately 85 $N/cm^2$ (123 psi). The limiting pressure differential for worn out circumferential segmented seals, rotating ring seals and simple labyrinths is approximately 40 $N/cm^2$ (58 psi).

Test program results indicated the effect of pressure differential on airflow was more significant than speed for circumferential segmented and conventional face seals. Airflow through the face seal decreased with increasing speed at a given air pressure. This is also the case with rotating ring seals and labyrinths since centrifugal force tends to close the gap as speed increases. The self-acting face seal airflow increased with speed as would be expected since the lift force increases with speed and therefore the leakage gap increases.

## SUMMARY OF RESULTS

Four types of shaft seals were evaluated under simulated gas turbine operating conditions which included pressure to 148 $N/cm^2$ (215 psia). The results of this experimental evaluation revealed the following:

1. The self-acting face seal operated without rubbing contact. This was evidenced by lack of wear. Of particular interest was the successful operation at 54 600 rpm (183 m/s (600 ft/sec)); this was taken as evidence that the gas film stiffness was high enough to prevent rubbing contact under high inertia force conditions.

2. Self-acting face seal leakage was significantly lower than that of the three conventional seal types and less than the maximum judged allowable for advanced engine systems.

3. Conventional contact seals may not be satisfactory in future advanced engines because of excessive airflow.

a. Airflow through worn out circumferential segmented seals, rotating ring seals, and simple labyrinths is comparable for a given air-to-oil pressure differential. At pressure differentials above 40 $N/cm^2$ (58 psi). airflow through these seal configurations was considered excessive.

b. The circumferential segmented seal configuration operated well at moderate conditions, but at air-to-oil pressure differentials above approximately 41.4 $N/cm^2$ (60 psi) and speeds above approximately 107 m/sec (350 ft/sec), it wore excessively and eventually operated as a labyrinth.

c. Of the conventional seals tested, the face seal configuration was most successful at limiting airflow, however, at air-to-oil pressure differentials above approximately 85 $N/cm^2$ (123 psi), airflow was considered excessive.

## REFERENCES

1. Parks, A. J., McKibbin, R. H., Ng, C. C. W., and Slayton, R. M., "Development of Main-Shaft Seals for Advanced Air Breathing Propulsion Systems," Pratt & Whitney Aircraft, Rep. PWA-3161 (NASA CR-72338), August, 1967.

2. Povinelli, V. P., and McKibbin, A. H., "Development of Main-Shaft Seals for Advanced Air Breathing Propulsion Systems, Phase II," Pratt & Whitney Aircraft, Rep. PWA-3933 (NASA CR-72737), June, 1970.

3. Ludwig, L. P., and Johnson, R. L., "Design Study of Shaft Face Seal With Self-Acting Lift Augmentation. III - Mechanical Components," NASA TN D-6164, 1971.

4. Ludwig, L. P., Zuk, J., and Johnson, R. L., "Design Study of Shaft Face Seal With Self-Acting Lift Augmentation. IV - Force Balance," NASA TN D-6568, 1972.

5. Zuk, J., Ludwig, L. P., and Johnson, R. L., "Quasi-One-Dimensional Compressible Flow Across Face Seals and Narrow Slots. I - Analysis," NASA TN D-6668, 1972.

6. Zuk, J., and Ludwig, L. P., "Investigation of Isothermal, Compressible Flow Across a Rotating Sealing Dam. I - Analysis," NASA TN D-5344, 1969.

7. Zuk, J., and Smith, P. J., "Computer Program for Viscous, Isothermal Compressible Flow Across a Sealing Dam With Small Tilt Angle," NASA TN D-5373, 1969.

8. Zuk, J., Ludwig, L. P., and Johnson, R. L., "Design Study of Shaft Face Seal With Self-Acting Lift Augmentation. I - Self-Acting Pad Geometry," NASA TN D-5744, 1970.

9. Povinelli, V. P., and McKibbin, A. H., "Development of Main-Shaft Seals for Advanced Air Breathing Propulsion Systems, Phase III," Pratt & Whitney Aircraft, Rep. PWA-4263 (NASA CR-72987), July, 1971.

10. Elli, A., "The Leakage of Steam Through Labyrinth Seals," Trans. ASME, 57, pp. 115-122, (1935).

## TABLE I . SELF-ACTING FACE SEAL EVALUATION

| rpm | Speed | | Air Pressure | | Cavity Pressure | | Airflow (Two Seals) | | | Seal Temperature | |
|---|---|---|---|---|---|---|---|---|---|---|---|
| | (m/s) | (ft/sec) | ($N/cm^2$ abs) | (psia) | ($N/cm^2$ abs) | (psia) | (kg/s) | (scfm) | (lb/sec) | (K) | (°F) |
| 27 300 | 91 | 300 | 34.3 | 49.7 | 10.5 | 15.2 | <.0006 | < 1 | <.0013 | 347 | 164 |
| 36 400 | 122 | 400 | 34.3 | 49.7 | 10.5 | 15.2 | <.0006 | < 1 | <.0013 | 373 | 212 |
| 45 500 | 152 | 500 | 34.3 | 49.7 | 11.5 | 16.7 | .0006 | 1.0 | .0013 | 393 | 247 |
| 27 300 | 91 | 300 | 54.4 | 78.7 | 10.5 | 15.2 | .0007 | 1.2 | .0015 | 358 | 185 |
| 36 400 | 122 | 400 | 55.0 | 79.7 | 11.5 | 16.7 | .0009 | 1.5 | .0019 | 380 | 224 |
| 45 500 | 152 | 500 | 55.0 | 79.7 | 11.9 | 17.2 | .0012 | 2.0 | .0026 | 398 | 256 |
| 27 300 | 91 | 300 | 79.1 | 114.7 | 11.5 | 16.7 | .0011 | 1.9 | .0024 | 373 | 212 |
| 36 400 | 122 | 400 | 79.1 | 114.7 | 11.6 | 16.9 | .0013 | 2.3 | .0029 | 385 | 234 |
| 45 500 | 152 | 500 | 79.1 | 114.7 | 12.5 | 18.2 | .0017 | 2.9 | .0037 | 402 | 262 |
| 27 300 | 91 | 300 | 103.0 | 149.7 | 11.9 | 17.2 | .0015 | 2.6 | .0033 | 380 | 223 |
| 36 400 | 122 | 400 | 103.0 | 149.7 | 12.2 | 17.7 | .0018 | 3.1 | .0040 | 396 | 253 |
| 45 500 | 152 | 500 | 103.0 | 149.7 | 12.9 | 18.7 | .0023 | 4.0 | .0051 | 412 | 282 |
| 27 300 | 91 | 300 | 34.3 | 49.7 | 10.8 | 15.7 | <.0006 | < 1 | <.0013 | 333 | 140 |
| 36 400 | 122 | 400 | 34.3 | 49.7 | 11.2 | 16.2 | <.0006 | < 1 | <.0013 | 352 | 174 |
| 45 500 | 152 | 500 | 34.3 | 49.7 | 11.2 | 16.2 | <.0006 | < 1 | <.0013 | 371 | 210 |
| 54 500 | 183 | 600 | 34.3 | 49.7 | 12.2 | 17.7 | .0011 | 1.9 | .0024 | 392 | 246 |
| 27 300 | 91 | 300 | 55.0 | 79.7 | 11.2 | 16.2 | .0008 | 1.3 | .0017 | 348 | 166 |
| 36 400 | 122 | 400 | 55.0 | 79.7 | 11.5 | 16.7 | .0009 | 1.5 | .0019 | 366 | 200 |
| 45 500 | 152 | 500 | 55.0 | 79.7 | 11.9 | 17.2 | .0012 | 2.1 | .0027 | 381 | 226 |
| 54 500 | 183 | 600 | 55.0 | 79.7 | 12.9 | 18.7 | .0015 | 2.6 | .0033 | 396 | 253 |
| 27 300 | 91 | 300 | 103.0 | 149.7 | 11.9 | 17.2 | .0017 | 3.0 | .0038 | 359 | 186 |
| 36 400 | 122 | 400 | 103.0 | 149.7 | 12.2 | 17.7 | .0021 | 3.6 | .0046 | 373 | 212 |
| 45 500 | 152 | 500 | 103.0 | 149.7 | 13.6 | 19.7 | .0029 | 5.0 | .0064 | 387 | 237 |
| 54 500 | 183 | 600 | 103.0 | 149.7 | 15.0 | 21.7 | .0039 | 6.7 | .0085 | 400 | 260 |
| 27 300 | 91 | 300 | 123.9 | 179.7 | 12.5 | 18.2 | .0023 | 3.9 | .0050 | 364 | 196 |
| 36 400 | 122 | 400 | 123.9 | 179.7 | 13.2 | 19.2 | .0032 | 5.5 | .0070 | 373 | 212 |
| 45 500 | 152 | 500 | 123.9 | 179.7 | 14.3 | 20.7 | .0036 | 6.2 | .0079 | 386 | 236 |
| 54 500 | 183 | 600 | 123.9 | 179.7 | 16.3 | 23.7 | .0046 | 8.0 | .0102 | 402 | 263 |

TABLE II - TYPICAL OPERATING CONDITIONS DURING 150 HOUR ENDURANCE RUN

| rpm | Speed | | Air Pressure | | Cavity Pressure | | Airflow (2 seals) | | | Fwd Seal Temp. | | Aft Seal Temp. | |
|---|---|---|---|---|---|---|---|---|---|---|---|---|---|
| | (m/s) | (ft/sec) | ($N/cm^2$ abs) | (psia) | ($N/cm^2$ abs) | (psia) | (kg/s) | (scfm) | (lb/sec) | (K) | (°F) | (K) | (°F) |
| 41 000 | 137 | 450 | 103 | 149.7 | 18.4 | 26.7 | .006 | 9.5 | .013 | 378 | 220 | 377 | 219 |
| 41 000 | 137 | 450 | 103 | 149.7 | 18.4 | 26.7 | .006 | 9.2 | .013 | 394 | 250 | 386 | 234 |
| | | | | | Shut Down | | | | | | | | |
| 41 000 | 137 | 450 | 103 | 149.7 | 17.0 | 24.7 | .006 | 9.5 | .013 | 369 | 204 | 372 | 210 |
| 41 000 | 137 | 450 | 103 | 149.7 | 17.0 | 24.7 | .006 | 8.8 | .012 | 385 | 233 | 381 | 226 |
| 41 000 | 137 | 450 | 103 | 149.7 | 17.0 | 24.7 | .006 | 9.0 | .012 | 390 | 243 | 386 | 234 |
| 41 000 | 137 | 450 | 103 | 149.7 | 17.0 | 24.7 | .005 | 8.7 | .012 | 398 | 256 | 388 | 238 |
| 41 000 | 137 | 450 | 103 | 149.7 | 16.7 | 24.2 | .005 | 8.4 | .012 | 404 | 266 | 391 | 244 |
| 41 000 | 137 | 450 | 103 | 149.7 | 16.9 | 24.5 | .005 | 8.2 | .011 | 404 | 266 | 390 | 243 |
| 41 000 | 137 | 450 | 103 | 149.7 | 17.0 | 24.7 | .006 | 9.0 | .012 | 400 | 259 | 388 | 238 |
| | | | | | Shut Down | | | | | | | | |
| 41 000 | 137 | 450 | 103 | 149.7 | 17.0 | 24.7 | .005 | 8.7 | .012 | 367 | 200 | 368 | 202 |
| 41 000 | 137 | 450 | 103 | 149.7 | 17.0 | 24.7 | .006 | 8.9 | .012 | 382 | 227 | 378 | 220 |
| 41 000 | 137 | 450 | 103 | 149.7 | 17.0 | 24.7 | .005 | 8.7 | .012 | 395 | 251 | 386 | 234 |
| 41 000 | 137 | 450 | 103 | 149.7 | 17.0 | 24.7 | .005 | 8.4 | .012 | 400 | 259 | 388 | 238 |
| 41 000 | 137 | 450 | 103 | 149.7 | 17.0 | 24.7 | .005 | 8.4 | .012 | 401 | 260 | 388 | 238 |
| 41 000 | 137 | 450 | 103 | 149.7 | 17.0 | 24.7 | .005 | 8.4 | .012 | 401 | 260 | 388 | 239 |
| 43 200 | 145 | 475 | 103 | 149.7 | 17.0 | 24.7 | .005 | 8.6 | .012 | 405 | 268 | 393 | 247 |
| 43 200 | 145 | 475 | 103 | 149.7 | 17.0 | 24.7 | .005 | 8.7 | .012 | 406 | 270 | 393 | 247 |
| | | | | | Shut Down | | | | | | | | |
| 43 200 | 145 | 475 | 103 | 149.7 | 17.4 | 25.2 | .006 | 9.6 | .013 | 378 | 221 | 378 | 220 |
| 43 200 | 145 | 475 | 103 | 149.7 | 17.4 | 25.3 | .006 | 9.1 | .013 | 393 | 247 | 387 | 236 |
| 43 200 | 145 | 475 | 103 | 149.7 | 17.1 | 24.8 | .005 | 8.7 | .012 | 400 | 260 | 389 | 241 |
| 43 200 | 145 | 475 | 103 | 149.7 | 17.2 | 24.9 | .005 | 8.5 | .012 | 405 | 268 | 393 | 247 |
| 43 200 | 145 | 475 | 103 | 149.7 | 17.0 | 24.7 | .005 | 8.5 | .012 | 403 | 264 | 392 | 246 |
| 43 200 | 145 | 475 | 103 | 149.7 | 17.0 | 24.7 | .005 | 8.7 | .013 | 402 | 262 | 390 | 242 |
| 43 200 | 145 | 475 | 103 | 149.7 | 17.0 | 24.7 | .005 | 8.2 | .010 | 407 | 271 | 394 | 250 |
| | | | | | Shut Down | | | | | | | | |
| 43 200 | 145 | 475 | 103 | 149.7 | 17.4 | 25.2 | .006 | 9.6 | .013 | 377 | 219 | 377 | 218 |
| 43 200 | 145 | 475 | 103 | 149.7 | 17.4 | 25.2 | .006 | 9.4 | .013 | 392 | 246 | 384 | 232 |
| 43 200 | 145 | 475 | 103 | 149.7 | 17.1 | 24.8 | .006 | 9.1 | .013 | 402 | 262 | 389 | 240 |
| 43 200 | 145 | 475 | 103 | 149.7 | 17.0 | 24.7 | .006 | 8.9 | .012 | 405 | 267 | 390 | 242 |
| 43 200 | 145 | 475 | 103 | 149.7 | 17.0 | 24.7 | .006 | 9.0 | .012 | 406 | 270 | 391 | 244 |
| 43 200 | 145 | 475 | 103 | 149.7 | 17.0 | 24.7 | .006 | 8.9 | .012 | 407 | 272 | 392 | 246 |
| 43 200 | 145 | 475 | 103 | 149.7 | 17.2 | 24.9 | .006 | 10.0 | .014 | 397 | 255 | 387 | 236 |
| | | | | | Shut Down | | | | | | | | |
| 43 200 | 145 | 475 | 103 | 149.7 | 16.7 | 24.3 | .006 | 9.0 | .012 | 388 | 239 | 383 | 229 |
| 43 200 | 145 | 475 | 103 | 149.7 | 17.0 | 24.7 | .005 | 8.5 | .012 | 399 | 258 | 390 | 242 |
| 43 200 | 145 | 475 | 103 | 149.7 | 16.7 | 24.2 | .005 | 8.5 | .012 | 402 | 263 | 390 | 242 |
| 43 200 | 145 | 475 | 103 | 149.7 | 16.7 | 24.2 | .005 | 8.3 | .011 | 405 | 268 | 394 | 248 |
| 43 200 | 145 | 475 | 124 | 179.7 | 19.1 | 27.7 | .008 | 13.0 | .018 | 404 | 266 | 388 | 238 |
| 43 200 | 145 | 475 | 124 | 179.7 | 19.1 | 27.7 | .008 | 13.0 | .018 | 402 | 262 | 386 | 234 |
| 43 200 | 145 | 475 | 124 | 179.7 | 19.1 | 27.7 | .008 | 13.0 | .018 | 398 | 256 | 383 | 230 |
| | | | | | Shut Down | | | | | | | | |
| 43 200 | 145 | 475 | 124 | 179.7 | 18.4 | 26.7 | .008 | 13.0 | .018 | 394 | 249 | 380 | 225 |
| 43 200 | 145 | 475 | 124 | 179.7 | 19.1 | 27.7 | .008 | 13.0 | .018 | 396 | 253 | 379 | 222 |
| 43 200 | 145 | 475 | 124 | 179.7 | 20.1 | 28.2 | .008 | 13.0 | .018 | 392 | 246 | 377 | 218 |
| 43 200 | 145 | 475 | 124 | 179.7 | 20.1 | 28.2 | .008 | 13.0 | .018 | 390 | 244 | 377 | 219 |
| 43 200 | 145 | 475 | 124 | 179.7 | 19.2 | 27.8 | .008 | 13.0 | .018 | 391 | 245 | 378 | 220 |
| 43 200 | 145 | 475 | 124 | 179.7 | 19.1 | 27.7 | .008 | 13.0 | .018 | 391 | 245 | 378 | 220 |
| 43 200 | 145 | 475 | 124 | 179.7 | 20.1 | 28.2 | .008 | 13.0 | .018 | 394 | 250 | 379 | 223 |
| 43 200 | 145 | 475 | 124 | 179.7 | 19.1 | 27.7 | .008 | 13.0 | .018 | 394 | 250 | 379 | 223 |
| | | | | | Shut Down | | | | | | | | |
| 43 200 | 145 | 475 | 124 | 179.7 | 19.1 | 27.7 | .008 | 13.5 | .019 | 392 | 246 | 382 | 228 |
| 43 200 | 145 | 475 | 124 | 179.7 | 19.1 | 27.7 | .008 | 13.5 | .019 | 391 | 245 | 301 | 227 |
| 43 200 | 145 | 475 | 124 | 179.7 | 18.4 | 26.7 | .008 | 13.0 | .018 | 392 | 246 | 381 | 227 |
| 43 200 | 145 | 475 | 124 | 179.7 | 18.4 | 26.7 | .008 | 13.0 | .018 | 395 | 251 | 384 | 231 |

## TABLE III. TYPICAL FACE SEAL TEST DATA

| rpm | Speed (m/s) | Speed (ft/sec) | Air Pressure ($N/cm^2$ abs) | Air Pressure (psia) | Cavity Pressure ($N/cm^2$ abs) | Cavity Pressure (psia) | Airflow (Two Seals) (kg/s) | Airflow (Two Seals) (scfm) | Airflow (Two Seals) (lb/sec) | Seal Temperature (K) | Seal Temperature (°F) |
|---|---|---|---|---|---|---|---|---|---|---|---|
| 27 300 | 91 | 300 | 79.1 | 114.7 | 17.7 | 25.7 | .007 | 12.5 | .016 | 350 | 170 |
| 36 400 | 122 | 400 | 79.1 | 114.7 | 18.1 | 26.2 | .007 | 12 | .015 | 363 | 195 |
| 45 500 | 152 | 500 | 79.1 | 114.7 | 17 | 24.7 | .006 | 10 | .013 | 394 | 250 |
| 27 300 | 91 | 300 | 103 | 149.7 | 21.5 | 31.2 | .011 | 19 | .024 | 383 | 230 |
| 36 400 | 122 | 400 | 103 | 149.7 | 21.8 | 31.7 | .010 | 17.5 | .022 | 350 | 170 |
| 45 500 | 152 | 500 | 103 | 149.7 | 20.6 | 29.7 | .008 | 14.5 | .018 | 366 | 200 |
| 27 300 | 91 | 300 | 123.9 | 179.7 | 23.9 | 34.7 | .014 | 24 | .031 | 352 | 175 |
| 36 400 | 122 | 400 | 123.9 | 179.7 | 25.3 | 36.7 | .013 | 23 | .029 | 333 | 140 |
| 45 500 | 152 | 500 | 123.9 | 179.7 | 23.9 | 34.7 | .011 | 19 | .024 | 344 | 160 |
| 27 300 | 91 | 300 | 148.2 | 214.7 | 28.8 | 41.7 | .017 | 30 | .038 | 347 | 165 |
| 36 400 | 122 | 400 | 148.2 | 214.7 | 27.4 | 39.7 | .015 | 26 | .033 | 330 | 135 |
| 45 500 | 152 | 500 | 148.2 | 214.7 | 30.8 | 44.7 | .017 | 29 | .037 | 340 | 155 |
| 36 400 | 122 | 400 | 148.2 | 214.7 | 31.6 | 45.7 | .019 | 32.5 | .041 | 333 | 140 |
| 27 300 | 91 | 300 | 148.2 | 214.7 | 30.2 | 43.7 | 018 | 31.5 | .040 | 306 | 90 |
| 18 200 | 61 | 200 | 148.2 | 214.7 | 30.2 | 43.7 | .019 | 33.5 | .043 | 303 | 85 |
| 18 200 | 61 | 200 | 123.9 | 179.7 | 26.7 | 38.7 | .016 | 27 | .034 | 306 | 90 |
| 27 300 | 91 | 300 | 123.9 | 179.7 | 27.4 | 39.7 | .016 | 27.5 | .035 | 312 | 100 |
| 36 400 | 122 | 400 | 123.9 | 179.7 | 26.7 | 38.7 | .014 | 24.5 | .031 | 322 | 120 |
| 45 500 | 152 | 500 | 123.9 | 179.7 | 27.4 | 37.7 | .012 | 21.5 | .027 | 333 | 140 |
| 27 300 | 91 | 300 | 77.7 | 112.7 | 19.5 | 28.2 | .008 | 14.5 | .018 | - | - |
| 36 400 | 122 | 400 | 79.1 | 114.7 | 19.8 | 28.7 | .008 | 14 | .018 | - | - |
| 45 500 | 152 | 500 | 79.1 | 114.7 | 19.8 | 28.7 | .008 | 13 | .017 | - | - |
| 54 600 | 183 | 600 | 79.1 | 114.7 | 19.8 | 28.7 | .008 | 13 | .017 | - | - |
| 27 300 | 91 | 300 | 103 | 149.7 | 23.7 | 34.7 | .013 | 23 | .029 | - | - |
| 36 400 | 122 | 400 | 103 | 149.7 | 23.7 | 34.7 | .012 | 21 | .027 | - | - |
| 45 500 | 152 | 500 | 103 | 149.7 | 23.7 | 34.7 | .011 | 19 | .024 | - | - |
| 54 600 | 183 | 600 | 103 | 149.7 | 23.7 | 34.7 | .010 | 17 | .022 | - | - |
| 27 300 | 91 | 300 | 123.9 | 179.7 | 28.1 | 40.7 | .018 | 30.5 | .039 | - | - |
| 36 400 | 122 | 400 | 123.9 | 179.7 | 28.1 | 40.7 | .017 | 30 | .038 | - | - |
| 54 600 | 152 | 500 | 123.9 | 179.7 | 28.1 | 40.7 | .015 | 26.5 | .034 | - | - |
| 54 600 | 183 | 600 | 123.9 | 179.7 | 28.1 | 40.7 | .014 | 23.5 | .030 | - | - |
| 27 300 | 91 | 300 | 148.2 | 214.7 | 34.3 | 49.7 | .023 | 39. | .050 | - | - |
| 36 400 | 122 | 400 | 148.2 | 214.7 | 33.6 | 48.7 | .021 | 35.5 | .045 | - | - |
| 45 500 | 152 | 500 | 148.2 | 214.7 | 32.9 | 47.7 | .019 | 33 | .042 | - | - |
| 54 600 | 183 | 600 | 148.2 | 214.7 | 32.2 | 46.7 | .017 | 29.5 | .038 | - | - |
| 36 400 | 122 | 400 | 77 | 111.7 | 17.7 | 25.7 | .007 | 12 | .015 | - | - |
| 45 500 | 152 | 500 | 79.1 | 114.7 | 18.4 | 26.7 | .007 | 12 | .015 | - | - |
| 54 600 | 183 | 600 | 79.1 | 114.7 | 17.7 | 25.7 | .005 | 9.5 | .012 | - | - |
| 63 700 | 213 | 700 | 79.1 | 114.7 | 19.8 | 28.7 | .006 | 10.5 | .013 | - | - |
| 36 400 | 122 | 400 | 103 | 149.7 | 23.9 | 34.7 | .012 | 21.5 | .027 | - | - |
| 45 500 | 152 | 500 | 103 | 149.7 | 23.2 | 33.7 | .010 | 18 | .023 | - | - |
| 54 600 | 183 | 600 | 103 | 149.7 | 21.2 | 30.7 | .008 | 14 | .018 | - | - |
| 63 700 | 213 | 700 | 103 | 149.7 | 23.9 | 34.7 | .010 | 16.5 | .021 | - | - |
| 36 400 | 122 | 400 | 123.9 | 179.7 | 31.6 | 45.7 | .020 | 34.5 | .044 | - | - |
| 45 500 | 152 | 500 | 123.9 | 179.7 | 31.6 | 45.7 | .017 | 30 | .038 | - | - |
| 54 600 | 183 | 600 | 123.9 | 179.7 | 28.8 | 41.7 | .015 | 26 | .033 | - | - |
| 63 700 | 213 | 700 | 123.9 | 179.7 | 29.5 | 42.7 | .014 | 24 | .031 | - | - |
| 36 400 | 122 | 400 | 148.2 | 214.7 | 36.4 | 52.7 | .025 | 43 | .055 | - | - |
| 45 500 | 152 | 500 | 148.2 | 214.7 | 35 | 50.7 | .023 | 39 | .050 | - | - |
| 54 600 | 183 | 600 | 148.2 | 214.7 | 34.3 | 49.7 | .021 | 35.5 | .045 | - | - |
| 63 700 | 213 | 700 | 148.2 | 214.7 | 30.8 | 44.7 | .016 | 27.5 | .035 | - | - |

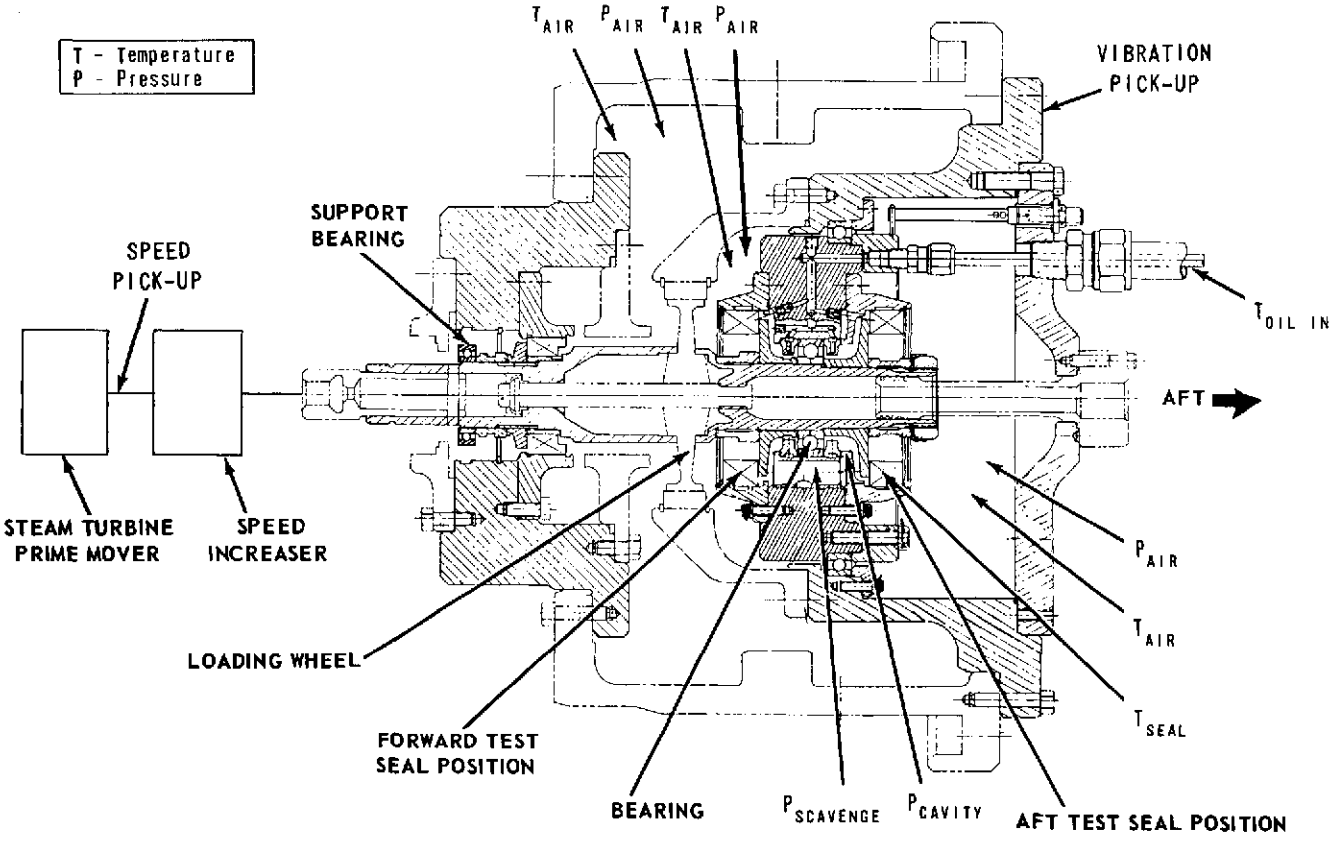


Figure 1. Test Vehicle and Instrumentation Plan.

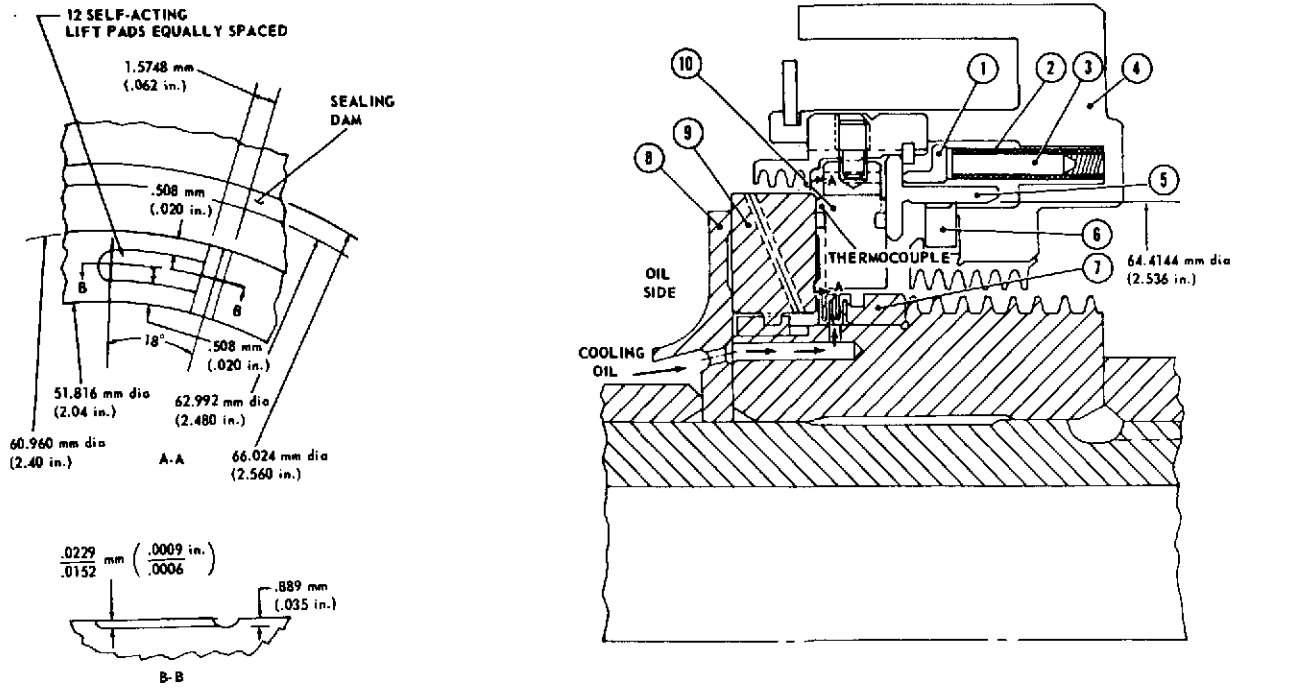


| | | | |
|---|---|---|---|
| 1. SPRING PLATE | INCONEL X750 | 6. PISTON RING | HIGH TEMPERATURE CARBON |
| 2. COMPRESSION SPRING | INCONEL X750 | 7. BELLOWS SPACER | INCONEL X750 |
| 3. SPRING PIN | 18-8 SST | 8. OIL DAM AND HEAT SHIELD | 440 SST |
| 4. HOUSING | INCONEL X750 | 9. FACE PLATE | 4340 FLAME SPRAYED WITH LINDE LCIC (CHROME CARBIDE) |
| 5. CARRIER | INCONEL X750 | 10. NOSEPIECE | HIGH TEMPERATURE CARBON AND TZM |

Figure 2. Self-Acting Face Seal Design.

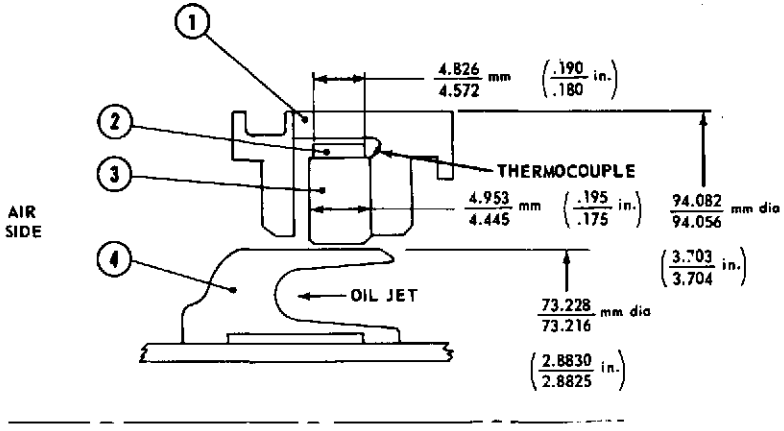


| | |
|---|---|
| 1. SEAL CASE | AMS 5610 |
| 2. RETAINING BAND | 431 SST |
| 3. CARBON RING | HIGH TEMPERATURE CARBON |
| 4. RUNNER | AMS 6382<br>CHROME PLATE PER AMS 2406 |

INTERFERENCE FIT BETWEEN RETAINING BAND AND CARBON RING: .356 mm (.014 in.) / .305 mm (.012 in.)

Figure 3. Rotating Ring Seal.

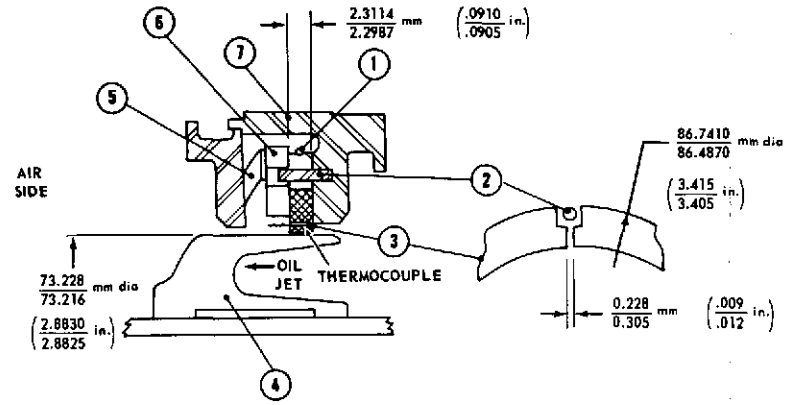


| | |
|---|---|
| 1. GARTER SPRING | AMS 5698<br>3.1 N LOAD (0.7 lb) |
| 2. ANTIROTATION PIN | AMS 5610 |
| 3. CARBON SEGMENT | HIGH TEMPERATURE CARBON |
| 4. RUNNER | AMS 6382 FLAME SPRAYED<br>WITH LCIC CHROME CARBIDE |
| 5. WAVE SPRING | AMS 5542<br>16.9 N LOAD (3.8 lb) |
| 6. SPACER | AMS 5610 |
| 7. SEAL CASE | AMS 5610 |

Figure 4. Circumferential Segmented Seal.

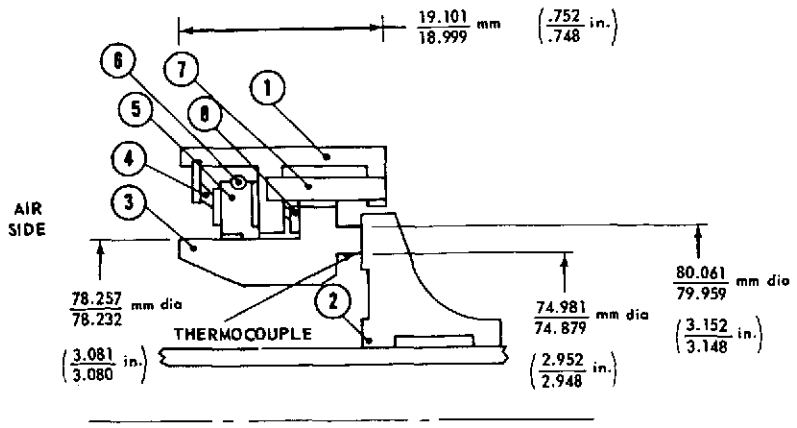


| | |
|---|---|
| 1. SEAL CASE | AMS 5610 |
| 2. FACE PLATE | AMS 6382 FLAME SPRAYED WITH LCIC CHROME CARBIDE COATING |
| 3. CARBON INSERT | HIGH TEMPERATURE CARBON |
| 4. WAVE SPRING | AMS 5542 |
| 5. SECONDARY SEAL | HIGH TEMPERATURE CARBON |
| 6. GARTER SPRING | AMS 5698<br>2.21 N LOAD (.5 lb) |
| 7. ANTIROTATION PIN | AMS 5610 |
| 8. WAVE SPRING | AMS 5542<br>TOTAL WAVE SPRING LOAD<br>31.1 N (7 lb) |

Figure 5. Face Seal.

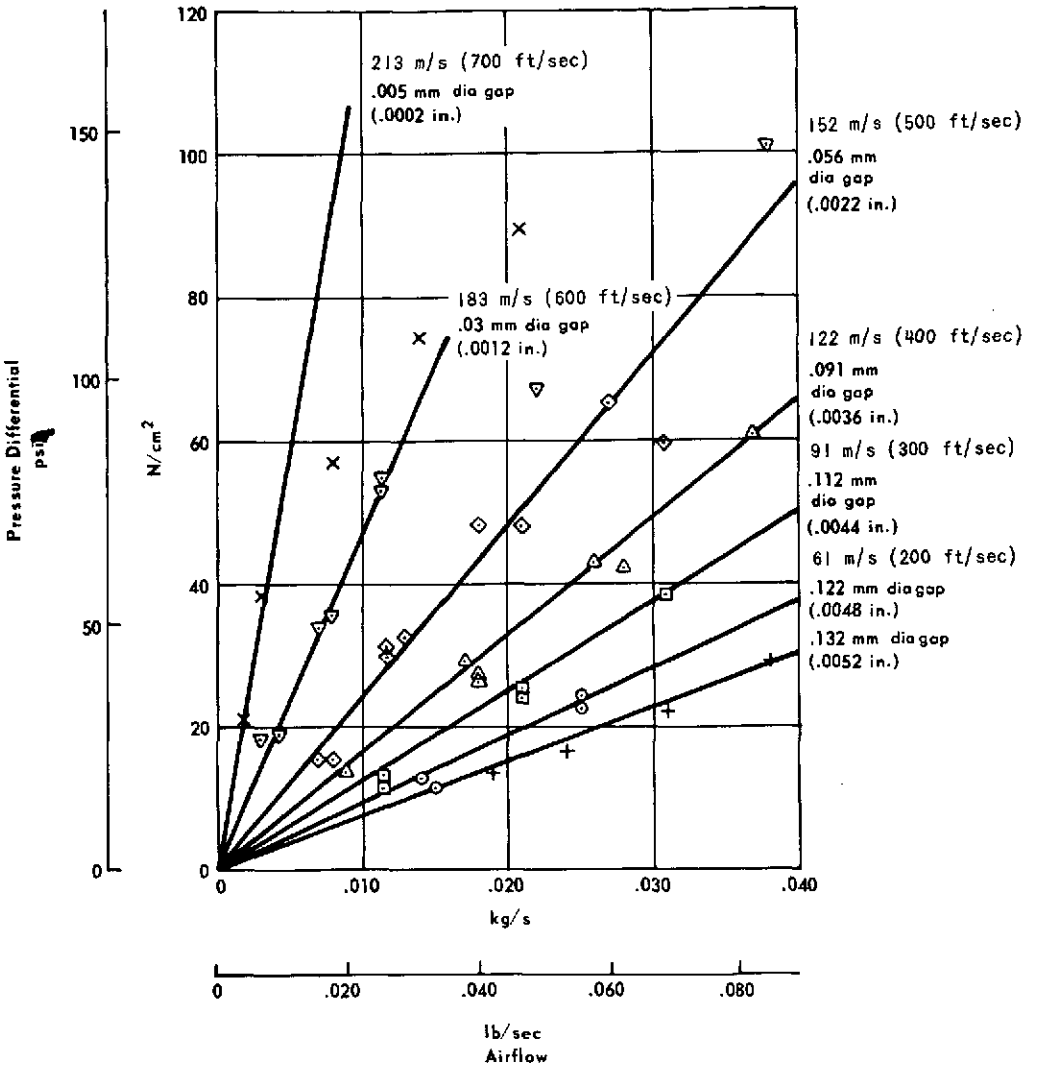


Figure 6. Airflow Through Two Rotating Ring Seals Versus Pressure Differential Between Air Side and Oil Side.

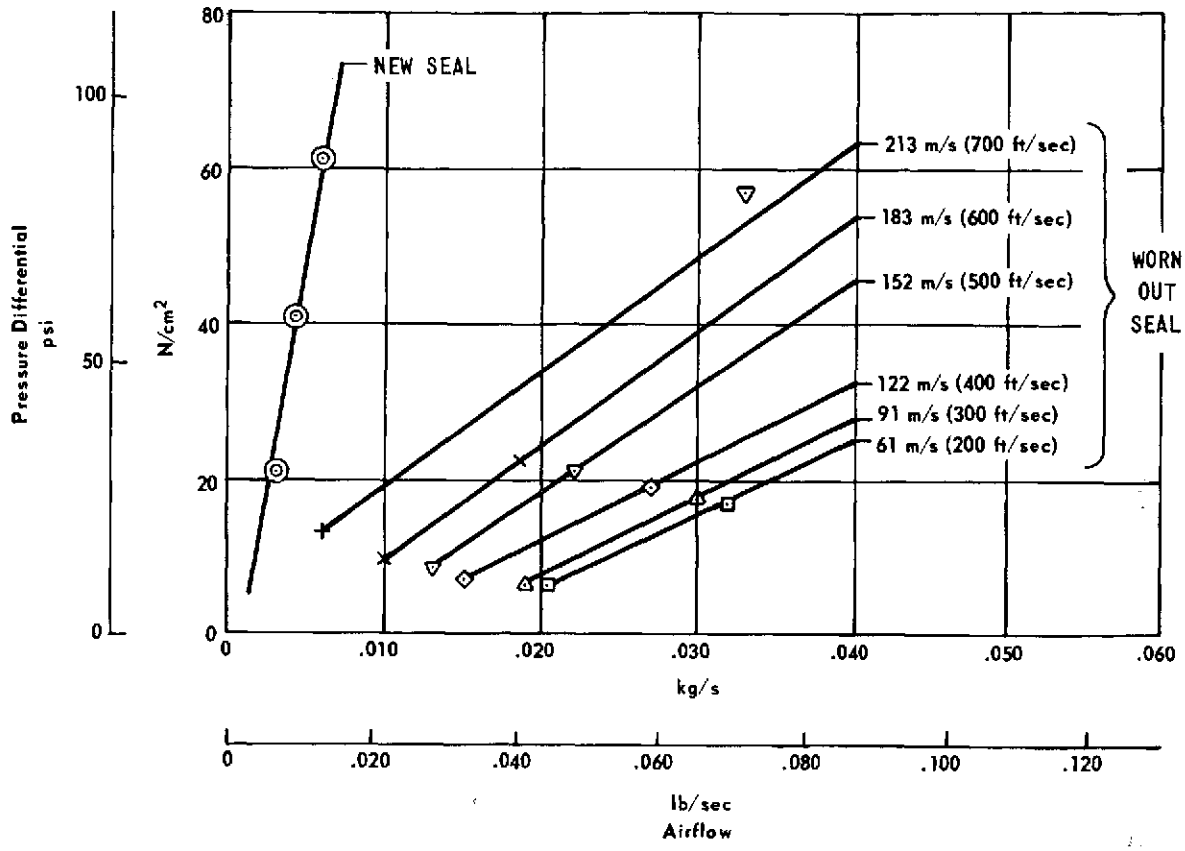


**Figure 7.** Airflow Through Two Circumferential Segmented Seals Versus Pressure Differential Between Air Side and Oil Side.

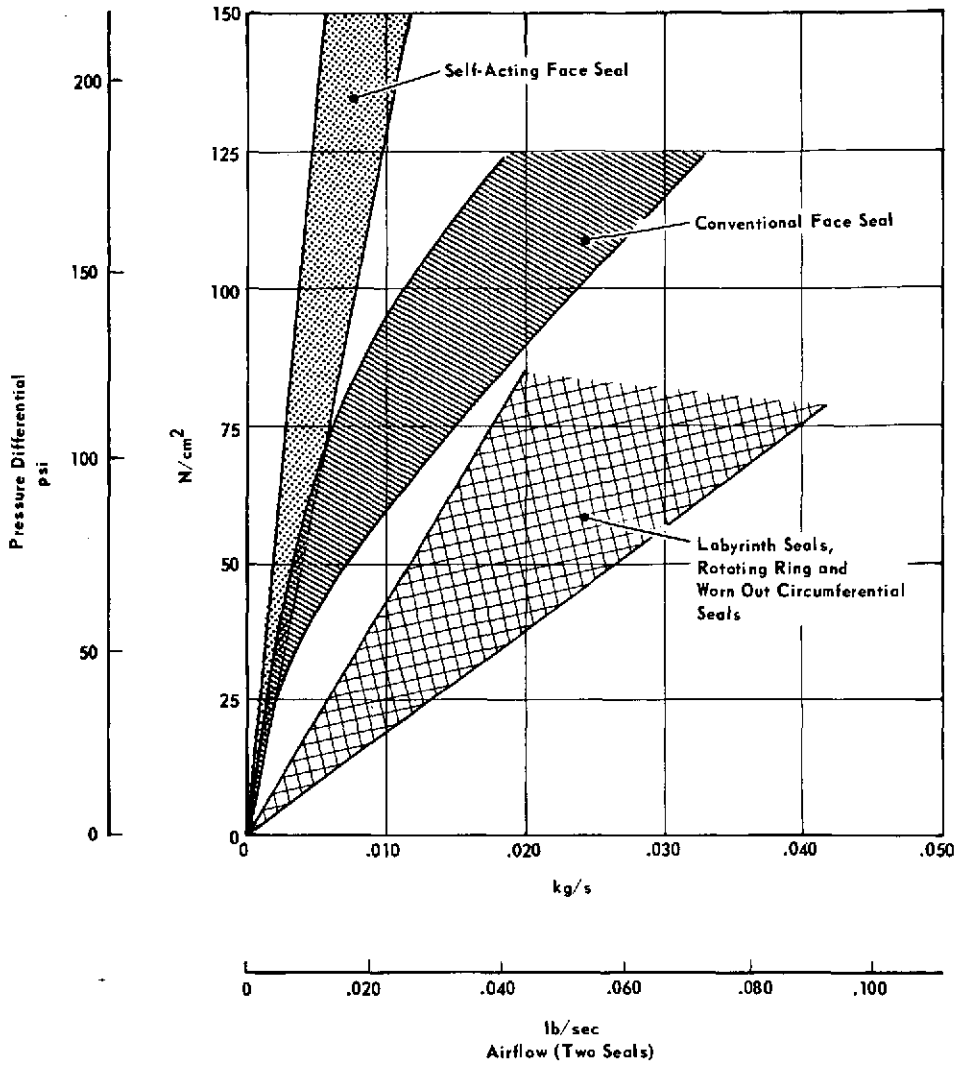


Figure 8. Comparison of Seal Configurations.

NASA-Lewis